

Role of Soil Moisture in the Seasonal Progress of the Asian Summer Monsoon

Masayoshi FUTAMI*, Masamichi OHBA**, and Hiroaki UEDA***

Abstract

In the seasonal evolution of the Asian summer monsoon (ASM), soil moisture has an important role as a source of the subsequent rainfall. Contrasting to this positive feedback, enhanced convection and ensuing wet soil act to decrease the land surface temperature, which dumps the ASM intensity through attenuated thermal gradient between the Asiatic landmass and adjacent oceans. Taking into account these offsetting effects, we conducted an idealized GCM experiments, i.e., soil moisture fixed run and interactive run, to elucidate the role of the land surface in the first transition of ASM in mid-May and northward excursion of the Indian monsoon during the latter half of June.

Experiments indicate that enhancement of convection over the India and neighboring oceans in mid-May is intimately related to the land surface condition, while the role of soil moisture is not relatively clear in the northward excursion of rain belt over the Indian subcontinent in June.

Key words: Soil moisture, Asian summer monsoon, GCM, Seasonal evolution

1. Introduction

Time evolution of a general circulation leading to establishment of the Asia summer monsoon (hereafter, referred to as ASM) is a crucial mode of the global climate system.

There are two stepwise seasonal transition involved in the ASM during May and June (e.g., He *et al.* 1987; Wang and LinHo 2002). The monsoon rainfall commences firstly over the South China Sea in mid-May. Subsequently, enhancement of convection takes places over the India in June, which is closely associated with northward excursion of rain belt (Yasunari 1981; Xie and Saiki 1999).

It is widely recognized that the monsoon is manifested as a land-atmosphere-ocean interaction (e.g., Yasunari 2007). Land surface processes are thought to be an active component in a seasonal progress of the ASM, which requires careful modeling (Ferrenti *et al.* 1999). In

particular, a physical mechanism for the land-atmosphere interaction can be analyzed by considering role of soil moisture.

Inland drizzles act to moisten soil while wet ground in turn supplies moisture to sustain deep convection and rainfall. Early study by use of the general circulation model (GCM) suggests that this interaction between rainfall and soil moisture is a slow process, limiting a speed of northward penetration of the monsoon rain belt (Xie and Saiki 1999). Koster *et al.* (2000) indicates that in continental mid-latitudes during the summer, oceanic impacts on precipitation are small relative to soil moisture impact. Several studies have evaluated effects of land and ocean by use of GCMs (Lestari and Iwasaki 2006; Sud *et al.* 2002; Yang and Lau 1998).

Recently, Ueda *et al.* (2009) revealed that land memory and atmospheric transient with solar radiation are an important players for the seasonal evolution of ASM especially over the land regions.

However, the Ueda *et al.*'s land/solar effect is determined by the residual of the perpetual SST experiment, in other words, soil moisture effect (hereafter, referred to as SME) is not deduced explicitly.

Given that the contribution from land surface feedbacks on the seasonal migration of precipitation remains debatable, not well known, and currently under discussion. Thus, purpose of this study is to quantify the role of slowly varying states of soil moisture in determining the seasonal evolution of the ASM. Particularly we focused on contribution from land memory in the two climatological transition stages occurring in mid-May and mid-June. In order to remove other possible effects associated with the boundary conditions over oceans or solar radiation, simulations in holding soil moisture piecewise constant in time mode have been performed using an atmospheric GCM (AGCM). Methods are described in section 2. In section 3, result of this study is discussed. Summary of major findings of this study is presented in the final section.

2. Methods

2.1 Model and Data

The model used in this study is AGCM (Shibata *et al.* 1999) of MRI-CGCM2.3.2, an atmosphere-ocean coupled model developed by Meteorological Research Institute in Japan (Yukimoto *et al.* 2006). A dynamical framework of the AGCM is a spectral transform method, with a

* United Nations Development Programme - United Nations Volunteers Programme, La paz, Bolivia.

** Central Research Institute of Electric Power Industry, Environmental Science Research Laboratory, Abiko, Japan.

*** Graduate School of Life and Environmental Science, University of Tsukuba, Tsukuba, Japan.

horizontal resolution of T42 in wave truncation, and 64×128 (about 2.8×2.8 degrees grid spacing in latitude and longitude) in transformed Gaussian grid. A vertical configuration consists of a 30-layer sigma-pressure hybrid coordinate, with the top at 0.4 hPa. A land component of the AGCM is based on the Simple Biosphere (SiB) model (Sellers *et al.* 1986; Sato *et al.* 1989), that a soil structure is represented as three layers.

Observational data set used in this study is the daily NCEP/NCAR (National Center for Environmental Prediction/ National Center for Atmospheric Reserch) atmospheric reanalysis (Kalnay *et al.* 1996) on a 2.5° grid of winds data. We also utilized the pentad mean Climate Prediction Center (CPC) merged analysis of Precipitation (CMAP) on a 2.5° grid derived from satellite (Xie and Arkin 1996).

2.2 Experimental Design

Ueda *et al.* (2009) developed a method to separate the effect of SST from other effects on the stepwise monsoon transitions. In this study, we applied their method to soil moisture. Two kinds of experiments are conducted. In the first part, the AGCM is fully coupled with land processes, which is integrated from the first day of January through the end of December for 30 year. The archived data is daily mean which is referred to as CTL run. In the second part, we conducted an AGCM experiment with piecewise constant soil moisture (PCSM) for one year from January through December. In this run, the soil moisture parameters of each layer were kept fixed at value of 15th days of each month until 15th days of the next month. We did not conduct long term PCSM experiments because long integrations with time-constant soil moisture, longer than one month, are inadequate, for they ignore soil moisture changes associated with the monsoon transitions.

Since the purpose of this study is to clarify the quantitative contribution from soil moisture, the atmospheric simulations are forced with daily SST lineally interpolated from a monthly SST climatology. To suppress internal variability of the atmosphere, 10-member ensemble PCSM integrations are performed for the diagnosis.

We carried out two types comparison between the CTL run and PCSM run as follows to isolate time change impact of soil moisture on transitional stages of ASM from that of all other forcing (non-SME), such as time variation of SST, the seasonal variation of solar radiation and internal atmospheric dynamics (atmospheric transients). Following equations extract SME and non-SME in which δ denotes time difference.

$$\delta_{SMP} \Big|_{M/15}^{M+1/1} = [P_c(M \ 1/2) - P_p(M)] \quad (1)$$

$$\delta_{non-SMP} \Big|_{M/15}^{M+1/1} = [P_p(M) - P_c(M)] \quad (2)$$

$P_c(M)$: monthly average M/1 - M/31 for CTL

$P_c(M \ 1/2)$: monthly average M/16 - M+1/15 for CTL

$P_p(M)$: monthly average M/16 - M+1/15 for perpetual

The subscripts c, p and M denote the control, PCSM runs and month, respectively. Note that two types of monthly mean (e.g., 5/1-5/30; 5/16-6/15) need to be prepared from the control run based on daily output. P is precipitation, which may be replaced by other meteorological variable. $P_c(M \ 1/2)$ is monthly average from M/16 until M+1/15 while $P_p(M)$ is the monthly average for the same period with soil moisture fixed at M/15 values. Soil moisture value of $P_c(M \ 1/2)$, approximate the value at M+1/1. Thus 15 days change (M/16 until M+1/1) of soil moisture component is included in the difference of (1). While $P_c(M \ 1/2)$ and $P_p(M)$ share the same non-soil moisture components, and these components are canceled out. Hence the precipitation change in (1) represents soil moisture changes from M/16 until M+1/1. Likewise, soil moisture of $P_c(M)$, approximates the value at M/15. Therefore $P_p(M)$ and $P_c(M)$ share the same mean soil moisture at M/15, and their difference in (2) is characterized by the response to 15 days changes (M/16 until M+1/1) of non-soil moisture component because the soil moisture components are removed.

We discuss the contributions from SME and non-SME, respectively for the 15 days natural change (M/16 until M+1/1) in recognizable two transitions as a chaotic result of all land-atmosphere-ocean interaction. Analogously, the time evolution of the total effect can be deduced by use of the following formula.

$$\delta_{TotalP} \Big|_{M/15}^{M+1/1} = [P_c(M \ 1/2) - P_c(M)] \quad (3)$$

3. Result

3.1 Observational Aspect and Experimental Results

First we state the time evolution of organized precipitation and low-level winds based on the observational data. Figure 1 shows the latitude-time sections of pentad mean climate precipitation of CMAP over the South China Sea (110° - 120° E) and the Indian subcontinent (70° - 85° E). Black line shows a stage when rainfall in excess of 8 mm/day reaches 20° N. In Fig.1a, enhancement of precipitation begins over the South China Sea from mid-May, which is indicative of the planetary monsoon onset (Li and Yanai 1996) and/or the first transition (He *et al.* 1987). As the season progresses, the Indian summer monsoon commences in the first half of

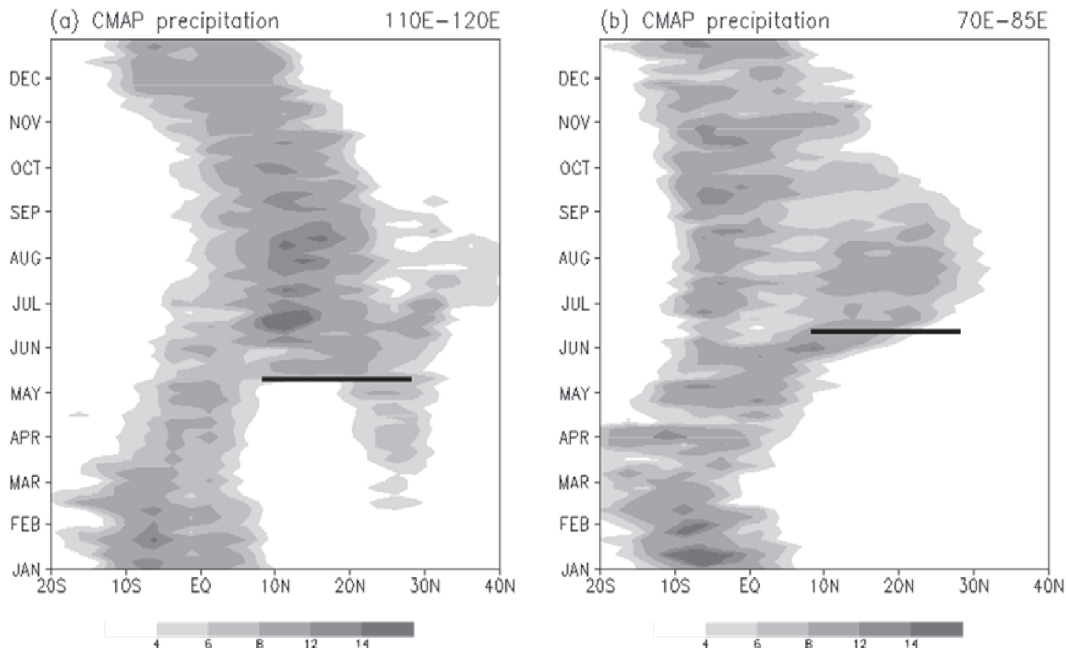


Fig.1. Latitude-time sections of CMAP precipitation (mm/day) averaged over (a) 70°E-85°E (Indian subcontinent), (b) 110°E-120°E (South China Sea).

June, which is followed by the northward penetration of rain belt over the Indian subcontinent (Fig. 1b). In the present study, we call the change in June as “second transition”.

Figure 2a and 2b plot differences for monthly average between M/16 and M+1/15 minus those between M/1 and M/31 with observation data. Figure 2c and 2d show 15 days differences of AGCM calculated from equation (3) using daily output of CTL. During the period of the first transition (5/16-6/1), southwesterly flows at low levels are well established over area from the Arabian Sea, Bay of Bengal and South China Sea, resulting in enhanced rains (Fig. 2a). The intense southwesterly flow near 15°N, 85°E is associated with a cyclonic depression developing over the Bay of Bengal (He *et al.* 1986). At the second transition, in the latter half of June (6/16-7/1), the intense southwesterly flow cover a broad belt extending from the Somalia coast to the Arabian Sea (Fig.2b). Corresponding to the manifestation of low level monsoon flow, distribution of negative (the Arabian Sea) and positive (the north India) anomaly on precipitation demonstrates northeastward displacement of convection toward the inland regions (Fig. 2b). The above features confirm that CTL bears a resemblance with the observation (Fig. 2c and 2d). One may notice that the absolute values of simulated CTL are different from the observation, however the overall features of CTL are well reproduced in the AGCM.

3.2 Role of Soil Moisture

In this subsection we mention a time varying impact of soil moisture component and non-soil moisture component during the two phases of monsoon. Figures 3a and 3b show SME on precipitation and horizontal wind at 850 hPa estimated from the equation (1). Be thoughtful what the differences of meteorological variables in these figures are due to the time change of soil moisture from M/16 until M+1/1. To confirm the statistical robustness, the ensemble mean signal to ensemble member noise ratio, $\{\Delta X\}/\sigma\Delta X$, is estimated from 10-members PCSM integrations for precipitation. A large ratio indicates that the signal stands out against to ensemble member variability (noise). White asterisks indicate that precipitation changes according to SME are robust feature (absolute values of signal-to-noise ratio for precipitation, in excess of 1.0). Figures 3c and 3d indicate the effect of some orbital parameters (non-SME) given by equation (2). The sum of differences of SME and non-SME equals to the differences of Figs. 2c and 2d.

At the first transition, SME contributes to the enhancement of southerly winds in the vicinity of the

Table 1. Precipitation changes (mm/day) in CTL, due to SME and Non-SME. The ratio to CTL run changes is in parentheses.

Period	mid-May	mid-June
Increment (mm/day)	4.78	3.53
SME (mm/day)	1.91 (39.8%)	-0.34 (-9.7%)
Non-SME (mm/day)	2.87 (60.2%)	3.87 (109.7%)

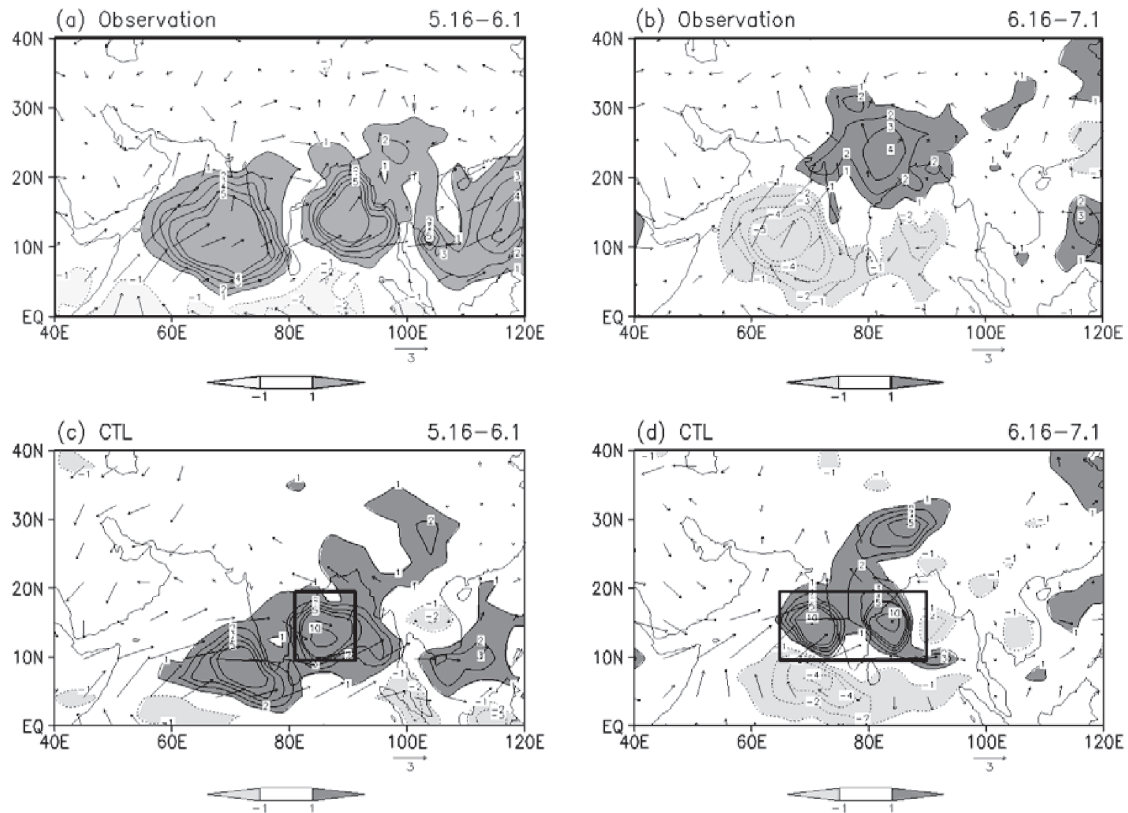


Fig.2. Seasonal changes (climatology) in CMAP precipitation (mm/day) and NCEP/NCAR reanalysis 850 hPa winds (m/s) in (a) first transition (5/16-6/1), (b) second transition (6/16-7/1). Under rank is same as up one but for CTL simulation of AGCM.

Indian subcontinent, particularly over the Bay of Bengal, which is accompanied by intensified convection (Fig. 3a). On the other hand, SME causes to suppress rainfall over the South China Sea and tropical Indian Ocean (Fig. 3a). In the meantime isolated non-SME excels to the intensification of southwesterly and growth of precipitation over the south Arabian Sea, Bay of Bengal and Malay Peninsula (Fig. 3c).

Once the Indian monsoon commences, SME reduces rainfall over the Bay of Bengal playing obstacle role in the northward excursion of rain belt (Fig. 3b). In this stage, there is no remarkable increase of the Indian monsoon rainfall by SME. It should be noted here that, non-SME is responsible for precipitation changes over the entire domain (Fig. 3d).

Solid squares in Figs. 2c and 2d show the core region of precipitation increase in excess of 10 mm/day of the total effect. The regional increment of precipitation due to the total effect, SME and non-SME is summarized in Table 1. Although non-SME functions as a main driver of seasonal evolution indicating the ratio to control run changes, 60.2% (mid-May) and 109.7% (mid-June), also SME is important player in the enhancement of convection,

accounting for 39.8% as for the first transition. On the other hand, the contribution from SME in the second transition is -9.7%, indicating suppressant effect for rainfall.

Figures 4a and 4b show SME on land surface temperature, geopotential height and wind field at 850 hPa, respectively. According to SME, a recognizable thermal gradient appears between Deccan Plateau and around Great Indian Desert. Moreover a cyclonic circulation is intensified over the Indian subcontinent at the first transition (Fig. 4a). However, like these aspects disappear at the mid-June (Fig. 4b). Hence it is plausible that enhancement of meridional thermal gradient within the Indian subcontinent by SME, is relevant to intensified rainfall in the southern part (Fig. 3a), which may be responsible for the anomalous moisture transport along 85°E and resultant active oceanic convection in early summer.

3.3 Global and Indian Effect

Delworth and Manabe (1989) suggested that mid-latitudes in the boreal summer are sensitive to potential contribution from soil moisture. Moreover, several recent

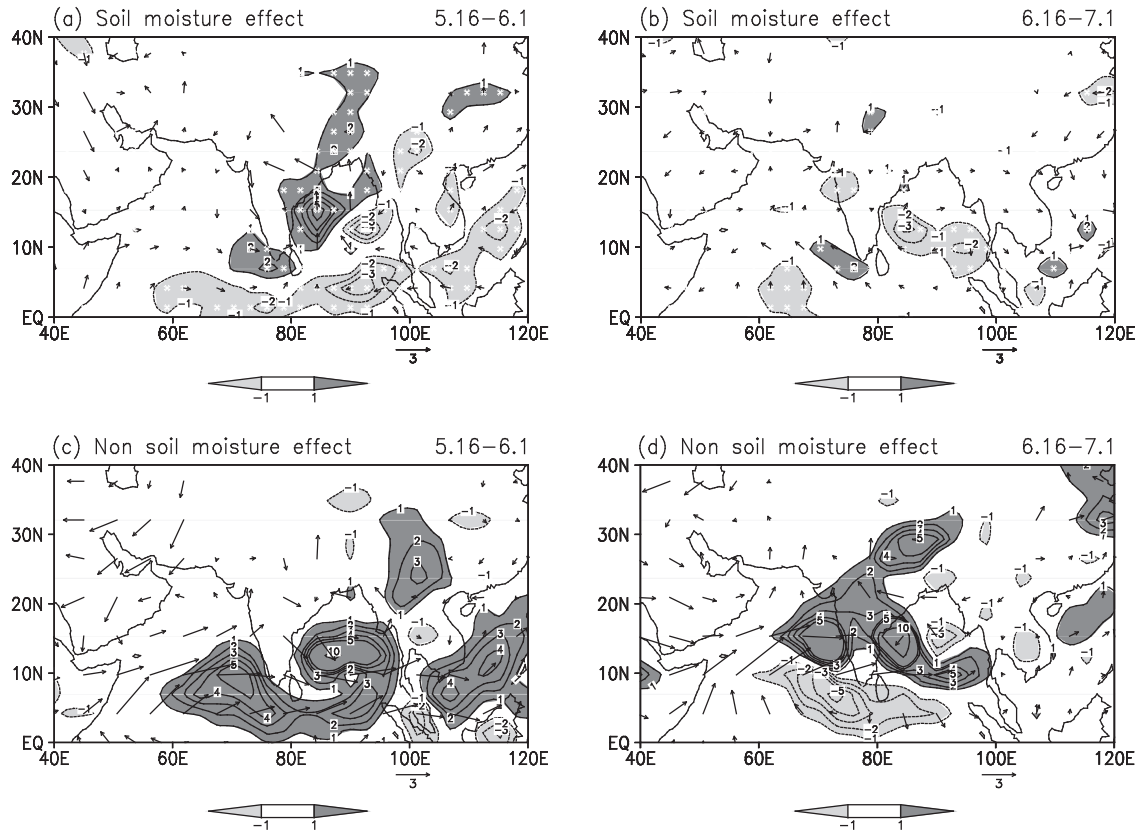


Fig. 3. Seasonal changes in precipitation (mm/day) and 850 hPa winds (m/s) due to SME [$P_r(M \frac{1}{2}) - P_r(M)$] at (a) first transition, (b) second transition. White asterisks indicate that precipitation changes according to SME are robust feature (absolute values of signal-to-noise ratio for precipitation, in excess of 1.0). Under rank is due to Non-SME [$P_r(M) - P_r(M)$].

researches emphasized that the impact of soil moisture is significant in the India based on numerical experiments (e.g., Douville *et al.* 2001; Koster *et al.* 2004). Therefore in this sub-section, we discuss SME for the seasonal march of precipitation by comparing Indian SME and global SME.

Figures 5a and 5b show spatial distribution of SME calculated from the PCSM experiment in which soil moisture is fixed only in the Northern part of India (20°N-30°N, 70°E-85°E) and hereafter referred to as NI-PCSM. The NI-PCSM simulations of 10 members ensemble are conducted as the global PCSM (hereafter referred to as All-PCSM) discussed in subsection 3.2.

In comparison with Fig. 3a, the SME of North Indian region (Fig. 5a) in precipitation and monsoon flow, reaches broad agreement at the first transition, in particular positive SME over Bay of Bengal and Indian subcontinent. As negative response of SME doesn't come out over the Indian Ocean in NI-PCSM, a similarity is recognized at the mid-June (Fig. 3b and Fig. 5b). Precipitation changes due to All-PCSM and NI-PCSM are shown in Table 2 (averaged in introduced box). The Table 2 reveals that there are quantitative resemblances between All-PCSM

and NI-PCSM (e.g., Mid-may: 39.8% and 36.6%). Hence these similarities suggest a possibility that North Indian's land condition affects considerably on the seasonal change of precipitation through remote influence.

4. Summary

In this study, we have analyzed the impact of the time-varying soil moisture on seasonal progress of ASM by performing idealized sensitivity experiments with the AGCM. In particular, we focused specifically on two distinct transitional stages of ASM occurring in mid-May and mid-June. The result of the experiments reveals that the land surface condition is an active factor to intensify convection over the Indian subcontinent and the west Bay of Bengal at the first transition. In contrast, SME on the precipitation at the second transition is not clear. Therefore

Table 2. Precipitation changes (mm/day) due to all land SME and North Indian SME. The ratio to CTL run changes is in parentheses.

Period	mid-May	mid-June
All-PCSM (mm/day)	1.91 (39.8%)	0.34 (-9.7%)
NI-PCSM (mm/day)	1.75 (36.6%)	0.19 (-5.4%)

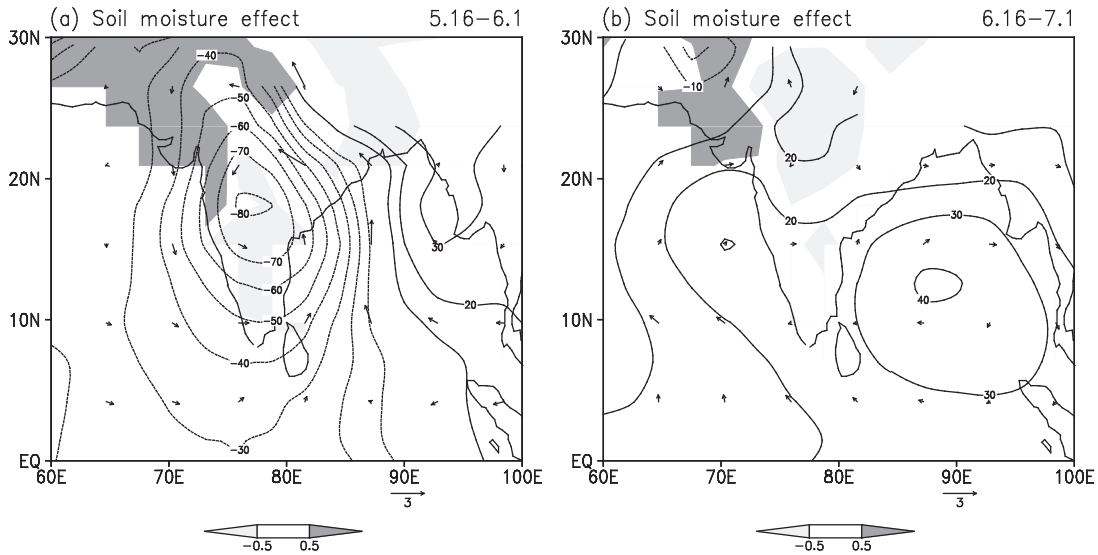


Fig. 4. Seasonal changes in geopotential height (m) and winds (m/s) at 850 hPa, land surface temperature (K) due to SME at (a) first transition, (b) second transition.

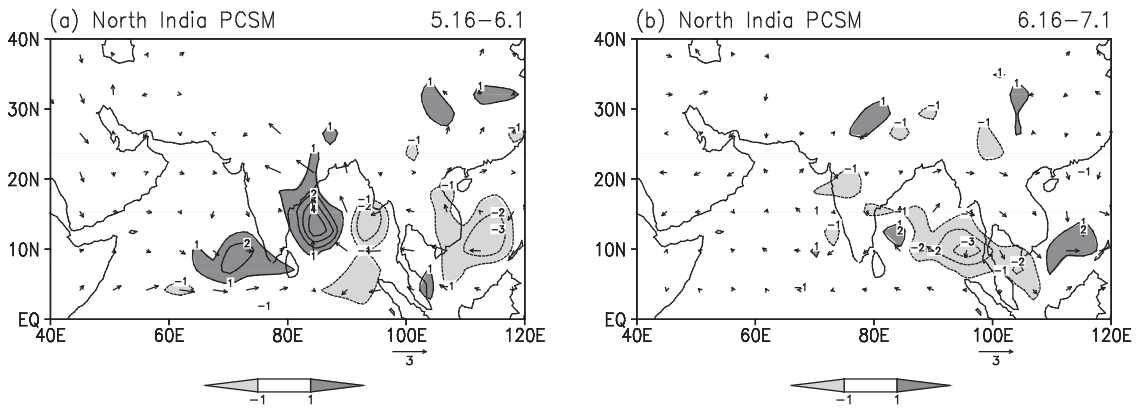


Fig. 5 SME calculated from NI-PCSM (Soil moisture is fixed only in North Indian region: 20°N-30°N, 70°E-85°E) on precipitation and 850 hPa wind, for (a) first transition, (b) second transition.

it could be conceivable that the northward propagating events over the second transition does not depend on the land-atmosphere interaction.

With isolating SST effect with piecewise constant SST experiment, Ueda *et al.* (2009) suggested that major changes in precipitation and circulation during the second half of June are due to land memory and atmospheric transient effects. According to our and Ueda *et al.*'s results, it is plausible that northward propagation event at second transition is mainly related to atmospheric transient.

Furthermore the similarity of convection's response between All-PCSM and NI-PCSM designates that the land memory of the North India has a substantial importance to discuss the role in the land surface condition on the seasonal progress of ASM.

Finally it should be pointed out that this method

assesses only the contribution from soil moisture changes during a short transition period (half month in this study), not the changes prior to the transition (Ueda *et al.* 2009). Also dynamical processes responsible of SME for the stepwise transitions of the monsoon circulation require additional investigations.

Acknowledgements

The first author would like to thank Dr. Shang-Ping Xie and Mr. Tomoshige Inoue for their kind discussion and technical support. This study was carried out under a cooperative agreement with MRI to use the AGCM.

References

Delworth, T. and S. Manabe (1988): The influence of potential evaporation on the variabilities of simulated

- soil wetness and climate. *J. Climate*, **1**, 523-547.
- Douville, H., F. Chauvin, and H. Broqua (2001): Influence of soil moisture on the Asian and African monsoons. Part I: Mean monsoon and daily precipitation. *J. Climate*, **14**, 2381-2403.
- Ferranti, L., J. M. Slingo, T. N. Palmer, and B. J. Hoskins (1999): The effects of land-surface feedbacks on the monsoon circulation. *Quart. J. Roy. Meteor. Soc.*, **125**, 1527-1550.
- He, H., J.W. McGinnis, Z. Song and M. Yanai (1987): Onset of the Asian Monsoon in 1979 and the effect of the Tibetan Plateau. *Mon. Wea. Rev.*, **115**, 1966-1995.
- Kalnay, E., and Coauthors (1996): The NCEP • NCAR 40-year reanalysis project. *Bull. Amer. Meteor. Soc.*, **77**, 437-471.
- Koster, R., M. J. Suarez, and M. Heiser (2000): Variance and predictability of precipitation at seasonal-to-interannual timescales. *J. Hydrometeorol.*, **1**, 26-46.
- Koster, R. (2002): Comparing the degree of land-atmosphere interaction in four atmospheric general circulation models. *J. Hydrometeorol.*, **3**, 363-375.
- Koster, R., and The Glace Team. (2004): Regions of strong coupling between soil moisture and precipitation. *Science*, **305**, 1138-1140.
- Lestari, R. K. and T. Iwasaki (2006): GCM study on the roles of the seasonal marches of the SST and land-sea thermal contrast in the onset of the Asian summer monsoon. *J. Meteor. Soc. Japan*, **84**, 69-83.
- Li, C., and M. Yanai (1996): The onset and interannual variability of the Asian summer monsoon in relation to land-sea thermal contrast. *J. Climate*, **9**, 358-375.
- Minoura, D., R. Kawamura, and T. Matsuura (2003): A mechanism of the onset of south Asian summer monsoon. *J. Meteor. Soc. Japan*, **81**, 563-580.
- Sato, N., P. J. Sellers, D. A. Randall, E. K. Schneider, J. Shukla, J. L. Kinter, Y.-T. Hou, and E. Alvertazzi (1989): Implementing the simple biosphere model in a general circulation model. *J. Atmos. Sci.*, **46**, 2757-2782.
- Sellers, P. J., Y. Mintz, Y.C. Sud, and A. Dlcher. (1986): A simple biosphere model (SiB) for use within general circulation models. *J. Atmos. Sci.*, **43**, 505-531.
- Shibata, K., H. Yoshimura, M. Ohizumi, M. Hosaka, and M. Sugi (1999): A simulation of troposphere, stratosphere and mesosphere with an MRI/JMA98 GCM. *Pap. Meteor. Geophy.*, **50**, 15-53.
- Sud, Y. C., G. K. Walker, V. M. Mehta, and W. K. M. Lau (2002): Relative importance of the annual cycles of sea surface temperature and solar irradiance for tropical circulation and precipitation: A climate model simulation study. *Earth Interactions*, **6**, 1-32.
- Ueda, H., M. Ohba, and S.-P. Xie (2009): Important factor for the development of the Asian-Northwest Pacific summer monsoon. *J. Climate*, **22**, 649-669.
- Wang, B. and Lin Ho (2002): Rainy season of the Asian-Pacific summer monsoon. *J. Climate*, **15**, 386-398.
- Xie, P. and P. Arkin (1997): Global precipitation: A 17 year monthly analysis based on gauge observations, satellite estimates and numerical model outputs. *Bull. Amer. Meteor. Soc.*, **78**, 2539-2558.
- Xie, S.-P. and N. Saiki (1999): Abrupt onset and slow seasonal evolution of summer monsoon in an idealized GCM simulation. *J. Meteor. Soc. Japan*, **77**, 949-968.
- Yang, S. and K.-M. Lau (1998): Influences of sea surface temperature and ground wetness on Asian summer monsoon. *J. Climate*, **11**, 3230-3246.
- Yasunari, T. (1981): Structure of an Indian summer monsoon system with around 40-day period. *J. Meteor. Soc. Japan*, **59**, 336-354.
- Yasunari, T. (2007): Role of land-atmosphere Interaction on Asian Monsoon climate. *J. Meteor. Soc. Japan*, **85B**, 55-75.
- Yukimoto, S., A. Noda, A. Kitoh, M. Hosaka, H. Yoshimura, T. Uchiyama, K. Shibata, O. Arakawa, and S. Kusunoki. (2006): Present-day climate and climate sensitivity in the Meteorological Research Institute Coupled GCM Version 2.3 (MRI-CGCM2.3). *J. Meteor. Soc. Japan*, **84**, 333-363.

Received 4 September 2009

Accepted 23 October 2009